SPARC-BD-04/001
20 January 2004

OFF-AXIS BEAM DYNAMICS IN THE HOMDYN CODE

M. Ferrario, V. Fusco, M. Migliorati, L. Palumbo, B. Spataro

INFN-LNF and Universita' di Roma "La Sapienza"

Abstract

When a bunch travels off axis across structures whose shape is not uniform, such as RF cavity or bellows, generates longitudinal and transverse wake fields. In addition transverse time dependent fields (like transverse RF components and wake fields) may induce correlated slice centroids displacement, so that each slice centroid motion is affected also by a different space charge force generated by the next slices.

We describe in this note the HOMDYN model including off axis beam dynamics. The analytical diffraction model for wake fields, due to Bane and Sands extended to a periodic structure (R.B. Palmer), is compared with the results of the numerical code ABCI and it is inserted in the HOMDYN code taking in to account also space charge forces acting on the slice centroids.

A preliminary study of the induced emittance and energy spread degradation is reported.

1 INTRODUCTION

When a bunch travels off axis across structures whose shape is not uniform, such as RF cavity or bellows, generates longitudinal and transverse wake fields. In addition transverse time dependent fields (like transverse RF components and wake fields) may induce correlated slice centroids displacement, so that each slice centroid motion is affected also by a different space charge force generated by the next slices.

We describe in this note the HOMDYN model including off axis beam dynamics. The analytical diffraction model for wake fields, due to Bane and Sands extended to a periodic structure (R.B. Palmer), is compared with the results of the numerical code ABCI and it is inserted in the HOMDYN code taking in to account also space charge forces acting on the slice centroids.

A preliminary study of the induced emittance and energy spread degradation is reported.

2 THE ANALYTICAL MODEL

The analytical model represents each structure as a pill-box cavity whose geometric dimensions, as shown in fig.2, are: *a* the beam pipe radius, *b* the cavity radius and *g* its length. When the bunch's rms length is much smaller than the beam pipe radius that is [1]

$$\sigma << a \tag{1}$$

methods of diffraction theory are used to calculate the impedance at high frequencies $\omega >> \omega_c$ where $\omega_c = 2.4\frac{c}{a}$ is the beam pipe cut off angular frequency.

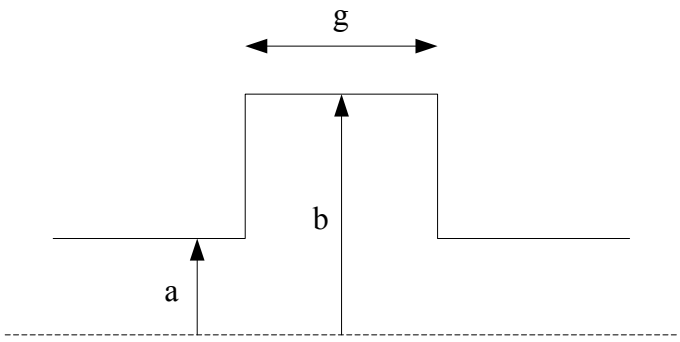

FIG. 2: Cavity like structure where *a* is the beam pipe radius, *b* is the cavity depth and *g* its length.

According to the diffraction theory, the impulsive longitudinal and transverse wake fields, in the high energy regime, $\sigma >> \frac{a}{\gamma}$, are respectively [2]

$$W_{\|0}(s) = \frac{Z_0 c}{\sqrt{2}\pi^2 a}\sqrt{\frac{g}{s}} \quad \left[\frac{\mathrm{V}}{\mathrm{C}}\right] \tag{2}$$

$$W_{\perp 0}(s) = \frac{2^{\frac{3}{2}} Z_0 c}{\pi^2 a^3} \sqrt{gs} \quad \left[\frac{\mathrm{V}}{\mathrm{C\,m}}\right] \tag{3}$$

where Z_0 is the characteristic impedance and s the longitudinal coordinate inside the bunch, being $s=0$ the bunch's head.

It's worth noting there is no energy dependence in the previous eq.(2) and eq.(1). The case of low energy regime were studied by Lawson [9] and Keil [10]. They stated there's a dependence of the energy loss, and so of the wake fields, from the γ. In [11], Henke analyzed the case of a charge passing trough a cavity with arbitrary velocity. He demonstrated the impedance decays with frequency faster for low energy than for high energy; then the Bane-Sand model represents an over estimation at low γ.

Both the longitudinal and transverse wakes do not depend on the cavity radius b. Infact some of the diffracted field, generated when the leading edge of the bunch enters the cavity, will propagate in the cavity; if the bunch's rms length σ is short as compared to the radius b of the cavity then the geometrical condition

$$g < \frac{(b-a)^2}{2\sigma} \tag{4}$$

is verified and the scattered field coming from the upper wall of the cavity will never reach the tail of the bunch itself: this is called "cavity regime" [5].

From eq.(2) and eq.(3), we get the longitudinal and transverse loss factors for a Gaussian bunch [2]

$$k_{\parallel} = \frac{Z_0 c}{4\pi^{5/2} a} \sqrt{\frac{g}{\sigma}} \left[\Gamma[1/4] - 4\left(\frac{\omega_c \sigma}{c}\right)^{\frac{1}{2}} \right] \quad \left[\frac{\mathrm{V}}{\mathrm{C}}\right] \tag{5}$$

$$k_{\perp} = \frac{4 Z_0 c}{\pi^3 a^3} \sqrt{g\sigma} \left[f(3/2) - \left(\frac{\omega_c \sigma}{c}\right)^{\frac{1}{2}} \right] \quad \left[\frac{\mathrm{V}}{\mathrm{Cm}}\right] \tag{6}$$

As σ goes to zero, we obtain the asymptotic formulas for the transverse and longitudinal loss factors [2]

$$k_{\parallel} = \frac{\Gamma(1/4) Z_0 c}{4\pi^{5/2} a} \sqrt{\frac{g}{\sigma}} \tag{7}$$

$$k_{\perp} = 4.36 \frac{Z_0 c}{\pi^3 a^3} \sqrt{g\sigma} \tag{8}$$

For a uniform distribution charge the longitudinal and transverse loss factors are

$$k_{\parallel} = \frac{4}{3\sqrt{2}} \frac{Z_0 c}{\pi^2 a} \sqrt{\frac{g}{l}} \left[\frac{V}{C}\right] \tag{9}$$

$$k_{\perp} = \frac{2^{\frac{7}{2}}}{15} \frac{Z_0 c \sqrt{\lg}}{\pi^2 a^3} \quad \left[\frac{V}{Cm}\right] \tag{10}$$

where *l* is the bunch's length.

The formulas shown above were obtained for one convolution. When the bunch travels along a periodic structure the total wake is not simply the summation of all convolution wakes; they combine to reduce their individual contribution as the beam moves along the structure [3]

$$k_N = k_0 \frac{2}{1+\sqrt{N}} \tag{11}$$

where k_N is the loss factor in the convolution *N* and k_0 is the longitudinal or transverse loss factor for one convolution. When the bunch reaches the N_{eq} convolution

$$N_{eq} = \frac{a^2}{2g(\sigma + \frac{2a}{\gamma})} \tag{12}$$

the individual wake remains constant and equal to the N_{eq} wake and the cumulative wake increases linearly with *N,* so the loss factor for the periodic structure, provided $N_{eq} >> 1$ and $\gamma^2 >> 1$, is given by [7]

$$k_{tot} = \left[\sum_{n=1}^{N_{eq}} \frac{2}{1+\sqrt{n}} + \frac{2(N_{tot} - N_{eq})}{1+\sqrt{N_{eq}}}\right] k_0 \tag{13}$$

where k_0 is either $k_{\parallel}$ or $k_{\perp}$ for one convolution.

3 COMPARISONS BEWTEEN THE ANALYTICAL MODEL AND THE CODE ABCI

The analytical model described in the preceding section is compared with ABCI's results. For example we considered two bellows configurations, for the emittance-meter experiment of the SPARC project

Bellow	a mm	b mm	g (compressed)mm	g (extended)mm
first	26.0	47.5	0.75	3.40
second	51.25	75.0	0.90	4.00

Tab.1: Two bellows dimensions considered for the SPARC project.

Note that for a bunch as the one used in the SPARC project (σ=*1mm*), these dimensions satisfy eq.(1) and eq.(4).

The plots in fig.3 represent the transverse and longitudinal loss factors as a function of the convolutions' number; the analytical model calculates them for a gaussian distribution bunch (eq.(5)-(8)) or a uniform distribution bunch (eq.(9) and eq.(10)) and for a squared shaped bellow; the code ABCI calculates them for a gaussian bunch and for a squared or

triangular shaped bellow. Excellent agreement is obtained between theory and numerical results, especially for the case of a gaussian bunch.

Eq.(7) and eq.(8) for a gaussian bunch are quite close to the numerical simulations, whilst eq.(9) and eq.(10), for a uniform bunch, almost coincide with the asymptotic eq.(7) and eq.(8)) of a gaussian bunch.

The second choice results to be more effective to damp wake fileds.

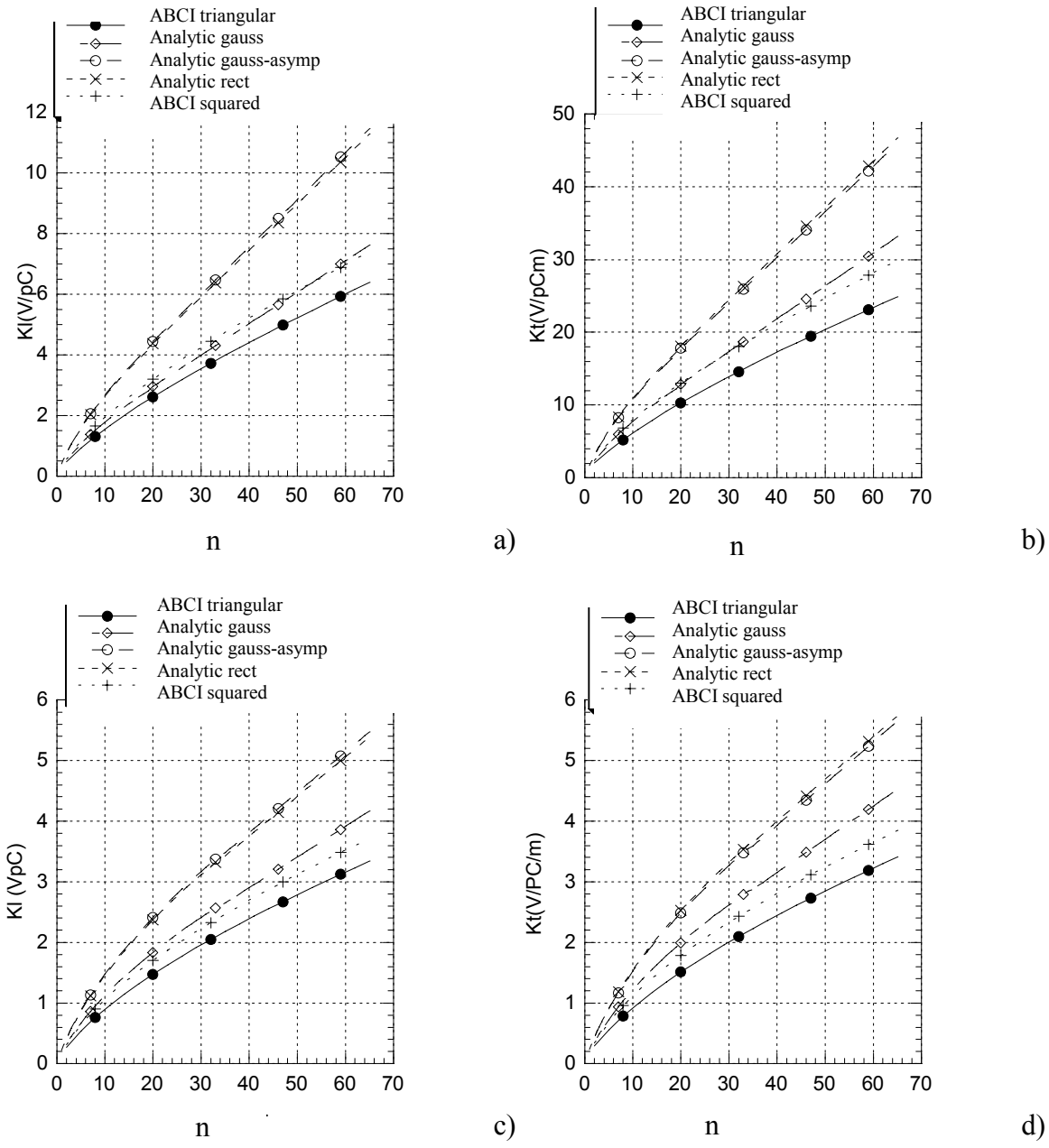

FIG. 3: Comparison between the ABCI code and the analytical formulas for the longitudinal (a, c) and the transverse (b, d) loss factor versus the number of convolutions for the first (a, b) and second (c, d) bellow. The bunch is *3.4 mm* long and its total charge is *1nC*.

4 ELECTRIC FIELD FOR N CONVOLUTIONS IN THE HOMDYN CODE

The HOMDYN code [8] describes a bunch as a uniformly charged cylinder, whose charge is *Q*, divided in cylindrical slices of radius *R*. The evolution, in the time domain, of the centroid x_c of each slice, is described transversally by

$$\ddot{x}_c + \beta\gamma^2\dot{\beta}\dot{x}_c + (K_s^{sol} + K_s^{rf})(x_c - x_{mis}) = \frac{2c^2 k_p}{\beta}\frac{x_c - \bar{x}}{R^2}\left(\frac{G(R,\zeta)}{\gamma^3} - (1+\beta^2)\frac{G(R,\xi)}{\gamma}\right) + \frac{e}{\gamma m}E_\perp(x^1{}_c - x_{mis}, s) \tag{14}$$

where x_{mis} is the element misalignment

On the left hand side of eq.(14)

$$K^{sol} = \left(\frac{eB_z(z)}{2m_0\gamma}\right)^2 \tag{15}$$

is the solenoid focusing gradient and

$$K^{rf} = \frac{e}{2\gamma m_0}\left(\frac{\partial E_z}{\partial z} + \frac{\beta}{c}\frac{\partial E_z}{\partial t}\right) \tag{16}$$

the RF focusing gradient expressed through the linear expansion off axis of the accelerating field $E_z = E_z(0,z,t)$.

Each slice's centroids can be transversally displaced from the nominal axis of x_c, fig.4. In this case it experiences a transverse deflection due to the transverse wake force and the space charge force produced by the neighbor slices. For this reason we included the space charge force (first term r. h. s.) where $G(R,\zeta)$ is [8]

$$G(R,\zeta) = \frac{1-\xi/l}{\sqrt{\left(\frac{R}{\gamma l}\right)^2 + \left(1-\frac{\zeta}{l}\right)^2}} + \frac{\zeta/l}{\sqrt{\left(\frac{R}{\gamma l}\right)^2 + \left(\frac{\zeta}{l}\right)^2}} \tag{17}$$

$\zeta = z_s - z_t$, $s = z_h - z_s$ (in fig.4 z_s is the position of a slice, z_t its tail and z_h its head), $\bar{x}$ is the average bunch's centroid, k_p is the beam perveance

$$k_p = \frac{I}{2I_0} \tag{18}$$

being I_0 the Alven current.

The second term on the right hand side of eq.(14) is the image charge from the cathode surface, whilst the wake force is represented by the last term.

Using the results of the previous section, the transverse wake field for one convolution is

$$E_\perp(x^1{}_c, s) = \frac{x^1{}_c}{g}\int_0^\infty \lambda(s-s')W_{\perp 0}(s')ds' \tag{19}$$

where $x^1{}_c$ is the displacement from the axis of the first slice.

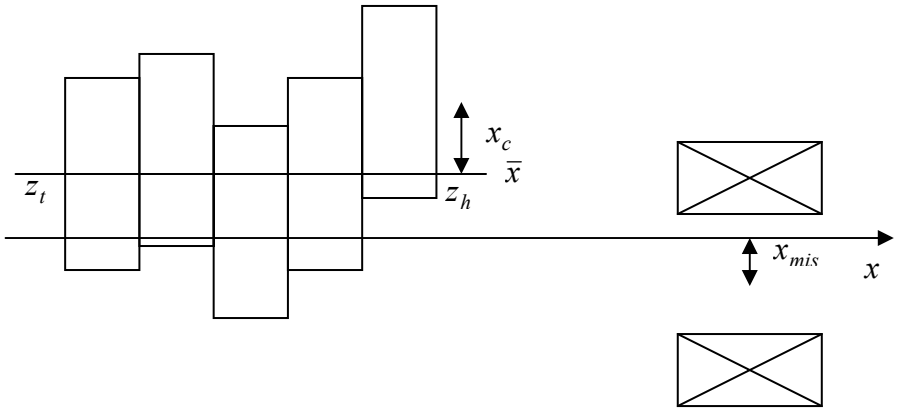

FIG. 4: Cylinder divided in cylindrical slices, representing a bunch in Homdyn. The displacement of each slice from the nominal axes is x_c.

When the bunch's charge is uniformly distributed

$$E_{\perp}(x^1{}_c, s) = \frac{x^1{}_c}{g}\int_0^s \frac{Q}{l} W_{\perp 0}(s')ds' = \frac{Q}{l}\frac{2^{5/2}}{3\pi^2 a^3 \varepsilon_0}\frac{s^{3/2}}{\sqrt{g}}x^1{}_c \quad \left[\frac{V}{m}\right] \tag{20}$$

The equations of the longitudinal motion of each slice's centroid in the Homdyn code, including acceleration, longitudinal wake and space charge force, are:

$$\dot{z}_c = \beta_c c \tag{21}$$

$$\dot{\beta}_c = \frac{e}{m_0 c\gamma^3}\left(E_z(z_s, t) + E_{\parallel}(s) + E_z^{sc} - \widetilde{E}_z^{sc}\right) \tag{22}$$

where $E^{sc}{}_z$

$$E_z^{sc} = \frac{Q}{4\pi\varepsilon_0 RL} H(\xi, R) \tag{23}$$

is the longitudinal space charge force, with

$$H(\xi, R) = \sqrt{(1-\xi/L)^2 + (R/\gamma L)^2} - \sqrt{(\xi/L)^2 + (R/\gamma L)^2} - |1-\xi/L| + |\xi/L| \tag{24}$$

$\widetilde{E}_z^{sc}$ is the contribution of the bunch image charge on the cathode.

The first term on the right hand side is the longitudinal wake, that is

$$E_{\parallel}(s) = \frac{1}{g}\int_0^{\infty} \lambda(s-s')W_{\parallel 0}(s')ds' \tag{25}$$

When the bunch's charge is uniformly distributed

$$E_{\parallel}(s) = \frac{1}{g}\int_0^s \frac{Q}{l} W_{\parallel 0}(s')ds' = \frac{Q}{l}\frac{2}{\sqrt{2}\pi^2 a\varepsilon_0}\sqrt{\frac{s}{g}} \quad \left[\frac{V}{m}\right] \tag{26}$$

The previous wake fields expressions are valid for one convolution. When the bunch is passing trough *n* convolutions we suppose the electric field follows the same law as the loss factor, that is eq.(11), provided that the conditions of section 2 apply; so we conclude the field in the n-th convolution is the one in the first convolution damped by the factor

$$f(n) = \frac{2}{1+\sqrt{n}} \tag{27}$$

Using a continuous form, being $n = \frac{z}{g}$

$$E(z,s) = E_0(s)\frac{2}{1+\sqrt{\frac{z}{g}}} \tag{28}$$

with the condition $g \le z \le N_{eq} g$, since for $z \le g$ the single cell field applies.

When $z \ge N_{eq} g$, according to section 2, the field reaches a steady value that we assume to be

$$E(z,s) = E_0(s)\frac{2}{1+\sqrt{\frac{z_{eq}}{g}}} = E_0(s)\frac{2}{1+\sqrt{N_{eq}}} \tag{29}$$

where

$$E_0(s) = \begin{cases} E_{\parallel}(s) \\ E_{\perp}(\Delta x, s) \end{cases} \tag{30}$$

is the longitudinal or the transverse electric field for one convolution (eq.(20) and eq.(26) respectively).
Both eq.(28) and eq.(29) can be inserted in the homdyn code that is in eq.(14) and eq.(22).

5 EMITTANCE AND ENERGY SPREAD COMPUTATION

The previous analitycal results, inserted in the homdyn code, can give an estimation of the emittance degradation and energy spread. The total rms emittance is calculated in the code as follow [8]

$$\varepsilon_{tot} = \sqrt{(\varepsilon_n^{th})^2 + (\varepsilon_n^{cor})^2} \tag{31}$$

that is it's a quadratic summation of the thermal emittance and the correlated emittance.
When all the slices lies on the same axis, the correlated emittance is simply given by [8]

$$\varepsilon_n^{cor} = \varepsilon_n^{E} = \frac{1}{4}\sqrt{< X^2 >< (\beta\gamma X')^2 > - < X\beta\gamma X' >^2} \tag{32}$$

where X is the bunch horizontal or vertical slice envelope, $X' = \frac{d}{dz}X$ and the average $\langle\ \rangle = \frac{1}{S}\sum_{s=1}^{S}$ is performed over the S slices.
On the contrary if the slices do not lie on the same axis then the correlated emittance is given by

$$(\varepsilon_n^{cor})^2 = \left\{(\varepsilon_n^E)^2 + (\varepsilon_n^C)^2 + (\varepsilon_n^{cross})^2\right\} \tag{33}$$

where

$$(\varepsilon_n^C)^2 = \left\langle (x_c - \bar{x})^2 \right\rangle \left\langle (\beta\gamma)^2 (x'_c - \bar{x}')^2 \right\rangle - \left\langle (x_c - \bar{x})\beta\gamma(x'_c - \bar{x}') \right\rangle^2 \tag{34}$$

is the centroid emittance and

$$(\varepsilon_n^{cross})^2 = \left\langle \frac{X^2}{4} \right\rangle \left\langle (\beta\gamma)^2 (x'_c - \bar{x}')^2 \right\rangle + \left\langle \frac{(\beta\gamma X')^2}{4} \right\rangle \left\langle (x_c - \bar{x})^2 \right\rangle - 2\left\langle \frac{X\beta\gamma X'}{4} \right\rangle \left\langle (x_c - \bar{x})\beta\gamma(x'_c - \bar{x}') \right\rangle \tag{35}$$

is a cross emittance term.

In the previous emittance equations x_c is the centroid of each slice, $x'_c = \frac{d}{dz} x_c$, $\bar{x} = \frac{1}{S}\sum_1^S x_c$ is the whole bunch's centroid, $\bar{x}' = \frac{d}{dz}\bar{x}$ and as above the average $\langle\ \rangle = \frac{1}{S}\sum_{s=1}^{S}$ is performed over the *S* slices.

6 EXAMPLES

The following plots represents the emittance evolution versus the longitudinal coordinates *z* calculated with the improved version of the Homdyn code for a bunch generated with an offset from the nominal trajectory of *1mm*. The bunch is traveling trough the gun, the solenoid gun of the SPARC project and a long corrugated bellows. Each plot represents three different situations: first we turn off the wake field, second we turn it on; in both cases the space charge is on. Finally we turn off the space charge. The tab.2 gives the emittance rate of change for the two bellow choice when the emittance reaches its maximum ($z \cong 1.5m$) and its minimum ($z \cong 2.0m$).

It's worth noting there is no much difference between the two corrugations' geometries. The reason is that, as fig.5 and tab.2 demonstrates, the real cause of the emittance degradation is the space charge on centroids rather than the wake fields.

Analytically we can compare the space charge force on the slices centroid and the wake force using eq.(14): the ratio between the transverse wake force and the space charge force for a uniformly charged bunch is

$$r = \frac{F^{Wake}}{F^{SpaceCharge}} = \frac{R^2}{3\pi a^2}\sqrt{\frac{2}{g}}\gamma^2 \frac{x^1{}_c}{|x_c - \bar{x}|}\frac{s^{3/2}}{G(\xi, R)} \tag{36}$$

and it gives an estimation of the strength of the wake as respect to the space charge.
Fig.6 shows the ratio between the wake force and the space charge force, *r*, versus the longitudinal coordinate inside the bunch, z_s, when γ and the structure geometry is fixed.

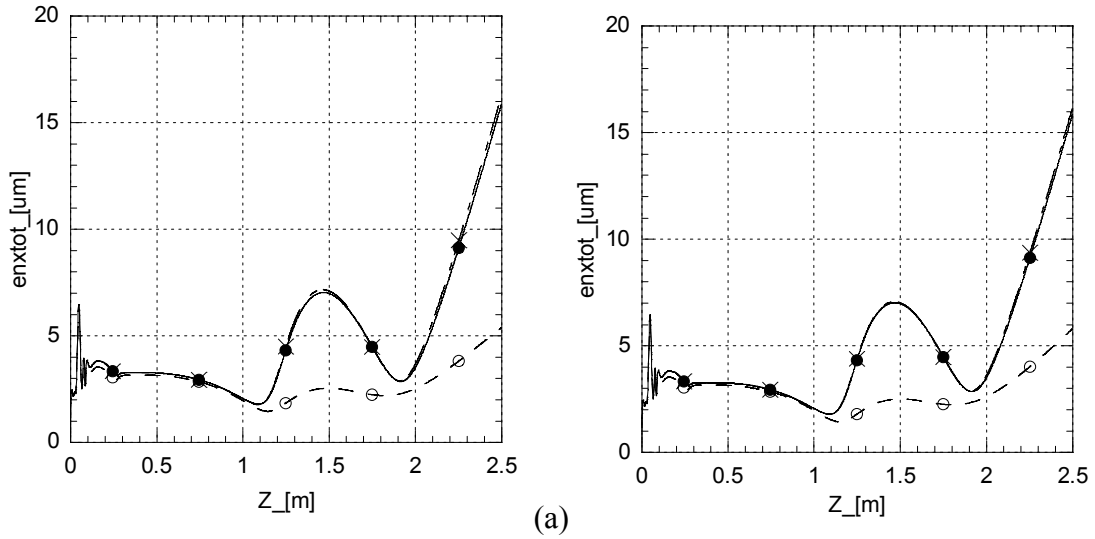

FIG. 5: Normalized emittances versus the longitudinal coordinate for an offset of *1mm* for the first (a) and the second (b) bellow geometries in the SPARC project, when the wake field is turned off (full circle), when the wake field is turned on(cross) and when the space charge on slices' centroid is turned off (empty circle) but the wake is still on.

When γ is small, that is the space charge still exists, the wake is smaller than the space charge force unless the slice's centroid is close to the whole bunch's centroid ($x_c - \bar{x} \to 0$).

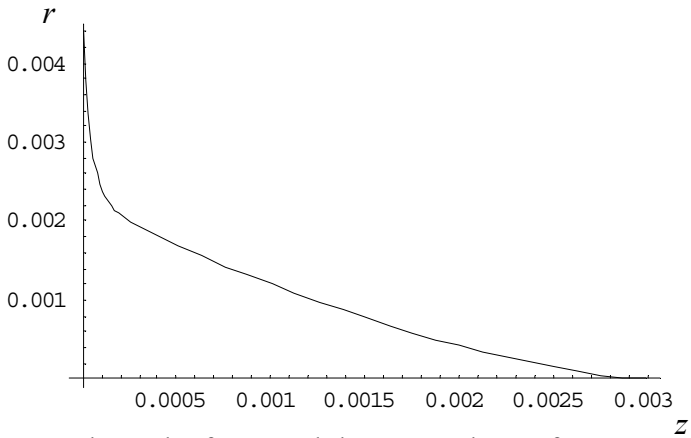

FIG. 6: Ratio between the wake force and the space charge force versus the longitudinal coordinate inside the bunch for $x_c^1 / |x_c - \bar{x}| = 1$. The structure geometry is the first bellow choice of tab.1 and the energy is $\gamma=12$.

Even if there's no difference in emittance degradation between the first and the second bellow choice the energy spread varies as can be seen in fig.8 and tab3. Homdyn computes the energy spread as

$$\frac{\Delta\gamma}{<\gamma>} = \frac{\sqrt{<(\gamma - <\gamma>)^2>}}{<\gamma>}$$

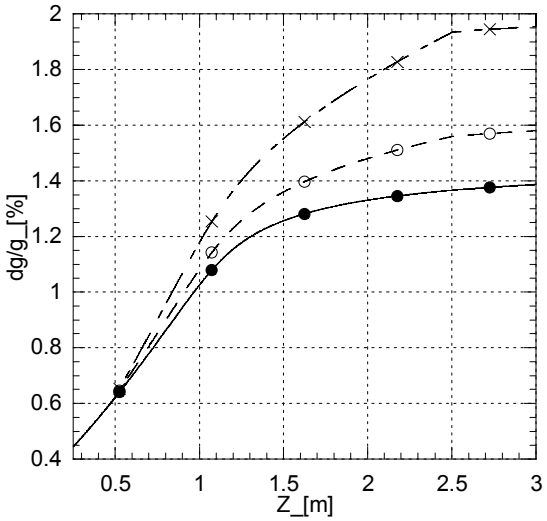

FIG. 8: Energy spread when there is no bellow (full circle) and when the first (cross) and second (empty circle) bellow are present.

	$\frac{\Delta\gamma}{\gamma}\%$
no bellow	1.3659
first bellow	1.9331
second bellow	1.5591

Tab.3: Bunch energy spread at the bellow exit (*z=2.5m*)

Finally the following plot represents each slice centroids as the bunch moves along the structure for an initial offset of *1mm*, with and without space charge; when the space charge is on, the centroids' displacement is driven by the space charge form factor [8].

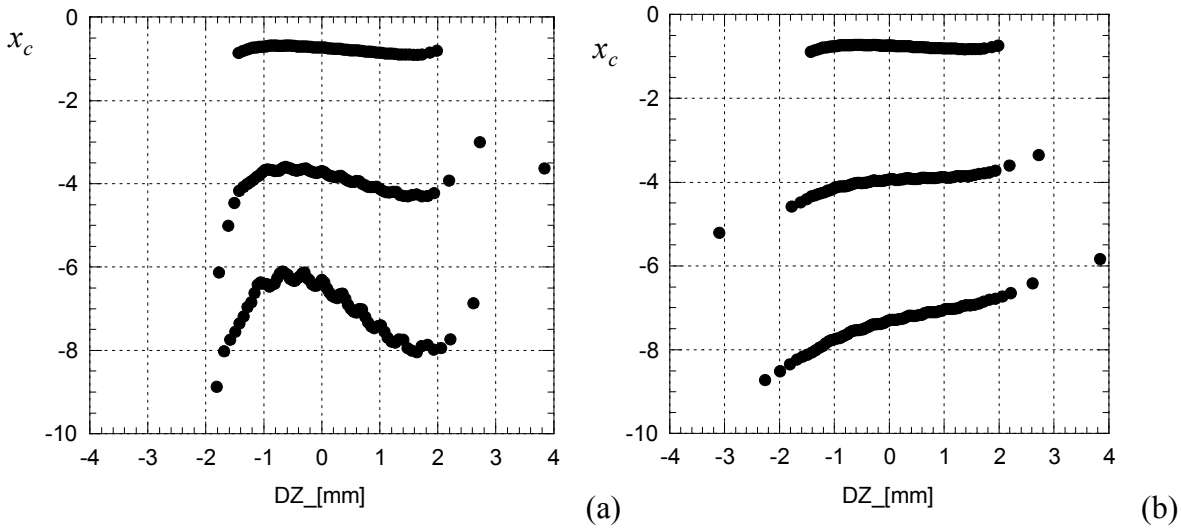

FIG. 9: Slice centroids as the bunch moves along the structure for an initial offset of *1mm* with (a) and without (b) space charge. In both cases the wake is on.

7 CONCLUSIONS

The wake fields of a short bunch passing throw a squared short cavity, sufficiently deep, are described at high frequency and high energy by a diffraction model due to Bane and Sands. This model can be extended in a simple way to a periodic structure as developed by R.B. Palmer. Such analytical model has been successfully compared with the results given by the code ABCI.

The obtained wake fields have been inserted in the homdyn code giving a dynamical estimation of theirs effect on the bunch. The centroid displacement from the axis gives rise to two more terms in the emittance analitycal evaluation: the centroid emittance and the cross term. This gives rise to a space charge force acting on centroids so when slices get misaligned the space charge on centroids becomes greater than the wake fields contributing to emittance growing.

8 ACKNOWLEDGEMENTS

We would like to thank D. Alesini and C. Ronsivalle for many helpful and interesting discussions.

9 REFERENCES

[1] L.Palumbo V.G. Vaccaro, M. Zobov, “Wake Fileds and Impedance”,

[2] K.Bane, M. Sands “Wake Fields of Very Short Bunches in an Accelerating Cavity”, SLAC-Pub-4441

[3] R.B. Palmer, “A Qualitative Study of wake Fields for Very Short Bunches”, SLAC PUB 4433 (1987)

[4] C. Limborg, YBatygin, M. Boscolo, M. Ferrario, V. Fusco, L. Giannessi, M. Quattromini, C. Ronsivalle, JP.Carneiro, K. Floetmann, ”Code Comparisons for Simulations of Photo-Injectors”, PAC03, SPARC_GE_03_002

[5] J.J. Bisognano “The Loss Parameter for Very Short Bunches”, CEBAF-PR-88-005

[6] B.W. Zotter, S.A. Kheifets, “Impedances and wakes in High-Energy Particle Accelerators”

[7] D.H Dowell “Bellows Induced Wakes in the Pepper Pot Experiment”, private comunication

[8] M.Ferrario et al., “Homdyn Study for the LCLS RF Photo-Injector”, SLAC-PUB 8400

[9] J.D. Lawson, “Radiation from a Ring Charge Passing Through a Resonator”, RHEL/M144 (1968)

[10] E. Keil, “Diffraction Radiation of Charged Rings Moving in a Corrugated Cylindrical Pipe”, NIM 100 (1972) 419-427

[11] H.Henke, “Point Charge Passing a Resonator with Beam Tubes”, CERN-LEP-RF/85-41